Tech Memo
AERO 2197

Tech Memo
AERO 2197

ROYAL AEROSPACE ESTABLISHMENT

Technical Memorandum

September 1990

A Simple Model of Vortex Flow Past a Slender Elliptic Cone at Incidence

by

M. Pidd
J. Pinkney
J. H. B. Smith

Procurement Executive, Ministry of Defence
Farnborough, Hampshire

CONDITIONS OF RELEASE

0086972 BR-115687

********** DRIC U

********** DRIC Y

Reports quoted are not necessarily available to members of the public or to commercial organisations.

ROYAL AEROSPACE ESTABLISHMENT

Technical Memorandum Aero 2197

Received for printing 8 October 1990

A SIMPLE MODEL OF VORTEX FLOW PAST A SLENDER ELLIPTIC CONE AT INCIDENCE

by

Joanne Pinkney*

M. Pidd

J. H. B. Smith

SUMMARY

The single line-vortex model of the separated flow past a slender pointed body of revolution at incidence is extended to elliptic cones, within the framework of slender-body theory, and maintaining lateral symmetry in the flow. An analytical solution is found for the limiting behaviour of the model when the vortices are weak. The angle of incidence above which solutions exist is found as a function of the axis ratio of the elliptic cross-section and the postulated location of the separation lines.

* Vacation Student, Summer 1989.

LIST OF CONTENTS

1 INTRODUCTION

When a slender pointed body is placed at a large angle of incidence, the boundary layers on its sides separate, and the resulting free shear layers roll up into vortices, which lie above the body in a direction between those of the body axis and the free stream. These vortices have an important influence on the aerodynamics of many combat aircraft and manoeuvring weapons.

It has been known for many years that the vortex flows of this kind that take place over sharp-edged wings can be represented successfully by inviscid models and there is evidence that the same is true for flows over round-edged wings and bodies, provided the location of the lines on the surface at which separation occurs can be specified. Since the noses of pointed bodies are approximately conical, knowledge of the vortex flow over cones is not only valuable in itself but also essential for understanding or calculating the development of the vortical flow along the body. The consideration of cones leads to an important simplification, since the supersonic inviscid flow over a cone is conical, in the sense that the velocity and pressure are constant along each ray through the apex. Moreover, if the apex angle is small enough for slender-body theory to apply, the lifting component of the flow field is conical at all Mach numbers.

Use of the slender-body approximation reduces the calculation of the lifting behaviour to the solution of a quasi-planar problem of incompressible flow in cross-flow planes normal to the flow direction or the body axis. The vortices formed by the rolled-up shear layers can then be represented most simply by the line (or point) vortices of planar, incompressible potential flow. A model of this kind was formulated by Bryson[1] for flow past bodies of revolution, and he presented numerical results for circular cones with a particular angular position of the separation line typical of turbulent flow. Additionally he showed that, as the angle of incidence, α, is reduced, the vortices reach the surface of the cone when

$$\frac{\alpha}{\delta} = 1.5 \operatorname{cosec} \theta_s \quad , \tag{1}$$

where δ is the semi-apex-angle of the cone and θ_s defines the positions of the symmetric separation lines OS_1 and OS_2 in Fig 1.

Moore[2] re-examined the behaviour of this model for circular cones. She found that, if θ_s is smaller than a critical angle of about 46°, there are two solutions for a range of values of α/δ smaller than those given by (1). For these values of θ_s, the model predicts that the initial movement of the vortices

away from the surface of the cone is associated with a decreasing angle of incidence, which is implausible in a model of the real flow. It emerges from recent calculations by Pidd[3] that solutions for values of α/δ less than 1.5 cosec δ_s are unstable to non-conical asymmetric disturbances, so equation (1) does, in some sense, provide a lower bound to the values of α/δ for which solutions of physical interest exist.

It is therefore of interest to apply this model to obtain a generalization of (1) to cones of elliptic cross-section. Before presenting the derivation of this generalization, we explain briefly why we believe the behaviour of so crude a flow model is relevant to present-day aerodynamics.

Much more representative models exist and their properties can be determined computationally, so what rôle remains for simple models? The more complete models that can be applied to problems of vortex flow are:

(a) the vortex-sheet model, which retains the framework of slender-body theory but provides a realistic representation of the shedding of circulation and of its subsequent convection, in the limit of infinite Reynolds number;

(b) the discretized Euler equation model, which more correctly represents effects of three-dimensionality and compressibility, but includes unreal effects of numerical diffusion, while excluding the effects of molecular or turbulent shear stresses; and

(c) the discretized Navier-Stokes equation model, with or without a model of turbulent stresses, which includes all the relevant physical effects (subject to the limitations of the turbulence model), perhaps masked by non-physical effects of numerical diffusion. A dramatic justification for the use of the simplest model, the one used in the present work, is provided by the way in which it has contributed to the understanding of asymmetric vortex flow past slender pointed bodies at incidence. The existence of asymmetric separated flow solutions of this model applied to a circular cone with specified symmetrically placed separation lines was demonstrated in 1981[4]. These solutions were used in the construction of asymmetric vortex sheet solutions, reported in 1982[5]. Solutions of the discretized Euler equations for conical supersonic flow, exhibiting properties like those of the vortex sheet solutions, appeared in 1988[6]. Early attempts to find Navier-Stokes solutions exhibiting gross asymmetry failed, but quasi-conical, grossly asymmetric solutions for supersonic speeds appeared in 1989[7]. All these solutions are consistent with a bifurcation of the symmetric solutions from the symmetric solution branch at a critical value of the parameter

α/δ , but the identification of the bifurcation locus has only been possible using the present simple model[3]. Moreover, the simple model has allowed the stability of the conical solutions to three-dimensional spatial disturbances to be determined[3]. With the vortex-sheet model, both stable and unstable solutions can be found, but so far it has not been possible to distinguish between them. The only solutions that can be obtained with the discretized models are those for which the numerical algorithm is stable, a condition which may or may not correspond with either physical stability or the mathematical stability of the solution. Finally, only the simple model gives a clear indication of its behaviour near the value of α/δ for which separation first arises, the particular aspect considered in the present work.

2 THE MODEL

2.1 Description

We list the assumptions made to obtain the highly-simplified model used in Refs 1 and 2 and herein. Firstly we assume that the body is sufficiently smooth and slender, and the angle of incidence is sufficiently small, for slender-body theory to apply to the flow outside the viscous regions at the free-stream Mach number of interest. Secondly, we assume that the Reynolds number is high enough for the displacement effects of the boundary layers and free shear layers to be negligible and for the rotational effects of the free shear layers which originate at separation to be represented adequately by vortex sheets. Finally we assume that each vortex sheet can be replaced by a combination of a line-vortex and feeding sheet, as described below. There is evidence from solutions for wing flows[3,4], that this assumption is reasonable when the vortices are small and weak.

According to slender-body theory, the disturbance velocity potential has two components, one of which is not relevant to the present model since it affects only the streamwise disturbance velocity. The other component is obtained as a solution of the two-dimensional form of Laplace's equation in the cross-flow plane, satisfying appropriate boundary conditions at infinity and the condition of no flow through the body surface. This component is itself the sum of two parts, one arising from the attached flow around the body and the other representing the effects of separation. The simplest representation of the effects of separation is chosen, in which the axial component of the rotation in each vortex sheet is concentrated into a single line-vortex, shown as OV_1 and OV_2 in Figs 1 and 2. The strength of the vortices is determined by applying a generalization of the Kutta condition, namely, that the flow at the separation line OS_1 or OS_2 is directed along the separation line. A proper inviscid model would involve vortex

sheets, rather than line vortices, and the pressure would be continuous across each sheet. In our simpler model we retain an integral form of this condition, that the cross-flow component of the total force acting on every elementary streamwise length of each 'vortex system' vanishes. The vortex system is the line vortex, OV, and the cut, or feeding sheet, OSV, which joins the line-vortex to the separation line. The cut is an essential part of the model since the strength of the vortex alters along its length in apparent violation of Kelvin's theorem. We can regard the cut as a feeding vortex sheet, conveying rotation from the body to the line-vortex. The vorticity vector in the cut lies in the cross-flow plane, so the divergence-free character of the vorticity field is maintained without affecting the cross-flow velocity.

2.2 Construction of velocity field

The body, an elliptic cone, is shown in Fig 2. We use the right-handed rectangular Cartesian axes shown, origin O at the cone vertex, Ox along its axis, Oy to starboard and Oz completing the system. The semi-axes of the elliptic cross-section are $a(x) = a'x$ and $b(x) = b'x$ parallel to the y and z axes respectively, where primes denote derivatives, constant in the present case. The onset flow has speed U and is inclined at an angle α to Ox. Since α is small, we can take its components as U parallel to Ox and αU parallel to Oz.

Let

$$Z = y + iz \tag{2}$$

be a complex variable in the cross-flow plane $x = \text{const}$. Then, if W is an analytic function of Z, its real part $\Re\{W\}$ is a solution of the two-dimensional form of Laplace's equation. We therefore seek a disturbance potential in the form of the real part of an analytic function which satisfies appropriate boundary conditions. We note that the cross-flow velocity components v parallel to Oy and w parallel to Oz are given by

$$v - iw = \frac{dW}{dZ} \quad . \tag{3}$$

The representation of the onset velocity then requires that

$$W \sim -i\alpha UZ \qquad \text{as} \quad Z \to \infty \; . \tag{4}$$

If the equation of the body surface is $S(x,y,z) = 0$, the condition of no flow through the surface is

$$US_x + vS_y + wS_z = 0 \quad , \tag{5}$$

assuming, as turns out to be the case, that u , the component of the disturbance velocity parallel to Ox , is small compared with U . The equation of the surface can be written conveniently as

$$S \equiv b^2(x)y^2 + a^2(x)z^2 - a^2(x)b^2(x) = 0 \quad ,$$

and so (5) becomes

$$U(bb'y^2 + aa'z^2 - a^2bb' - b^2aa') + b^2yv + a^2zw = 0 \quad . \tag{6}$$

Using ϕ , the eccentric angle, as a parameter on the elliptic cross-section, so that

$$y = a \cos \phi \quad , \quad z = b \sin \phi \quad , \tag{7}$$

we find the body boundary condition (6) becomes

$$bv \cos \phi + aw \sin \phi = U(ab' \sin^2\phi + a'b \cos^2\phi) \quad . \tag{8}$$

The normal direction to the ellipse in the cross-flow plane is $b \cos \phi : a \sin \phi$, so that v_n , the component of the cross-flow velocity normal to the elliptic cross-section, directed into the fluid, is

$$v_n = (bv \cos \phi + aw \sin \phi)/D \quad ; \tag{9}$$

$$D = (a^2 \sin^2\phi + b^2 \cos^2\phi)^{\frac{1}{2}} > 0 \quad . \tag{10}$$

Hence by (8) and (9)

$$v_n = U(ab' \sin^2\phi + a'b \cos^2\phi)/D \quad . \tag{11}$$

The attached flow is now given by the real part of the complex potential which satisfies (4) and (11). This is found by mapping the region of the Z-plane external to the ellipse on to the region of a ζ-plane external to a circle. If the circle is centred at the origin and has radius R , a general point on it is

$$\zeta = Re^{i\phi} = R(\cos\phi + i\sin\phi) \tag{12}$$

so that $\cos\phi = \frac{1}{2}(\zeta/R + R/\zeta)$ and $\sin\phi = \frac{1}{2}i(R/\zeta - \zeta/R)$. Hence, if

$$Z = \frac{a+b}{2}\frac{\zeta}{R} + \frac{a-b}{2}\frac{R}{\zeta}$$

the general point (12) on the circle corresponds to the general point (7) on the ellipse. We now choose

$$R = \tfrac{1}{2}(a+b) \tag{13}$$

so that $Z \sim \zeta$ at a large distance, and obtain the mapping

$$Z = \zeta + (a^2 - b^2)/4\zeta \quad . \tag{14}$$

The normal velocity required on the circle in the ζ-plane is

$$v_{n_\zeta} = v_n\left|\frac{dZ}{d\zeta}\right| \quad ,$$

so that, by (9) to (14),

$$v_{n_\zeta} = U(ab' + a'b + (a'b - ab')\cos 2\phi)/(a+b) \quad . \tag{15}$$

Since the body is a cone, we can write

$$b(x) = \tau a(x) \quad , \tag{16}$$

where τ is a constant, the thickness ratio of the cross-sections. Then (15) reduces to

$$\frac{v_{n_\zeta}}{U} = \frac{\tau aa'}{R} \quad .$$

This uniform normal velocity can be generated by a source at the origin of the ζ-plane of strength $2\pi Rv_{n_\zeta} = 2\pi U\tau aa'$. The appropriate behaviour (4) at a large distance requires, by (14), that

$$W \sim -i\alpha U\zeta$$

and a complex potential with this behaviour, generating no normal velocity on the circle, is

$$- i\alpha U(\zeta - R^2/\zeta) \quad .$$

Hence the complex potential of the attached flow, W_a, is obtained by adding these contributions:

$$W_a = \tau a a' U \log \zeta - i\alpha U(\zeta - R^2/\zeta) \quad . \tag{17}$$

To represent the effects of separation, we require the complex potential to behave like that of a line vortex of strength Γ near V_1, *ie* near $Z = Z_1$; and like that of a vortex of strength $-\Gamma$ near V_2, *ie* near $Z = -\bar{Z}_1$, where the overbar denotes the complex conjugate. The leading term in the behaviour of the flow at a large distance and the normal velocity on the body surface must not be affected. This is achieved by the introduction of line-vortices of strength Γ at $\zeta = \zeta_1$ and $-\Gamma$ at $\zeta = -\bar{\zeta}_1$, together with image vortices of strength $-\Gamma$ at $\zeta = R^2/\bar{\zeta}_1$ and Γ at $\zeta = -R^2/\zeta_1$, where ζ_1 is related to Z_1 through the mapping (14). Adding the appropriate complex potentials to (17) produces

$$W = \tau a a' U \log \zeta - i\alpha U\left(\zeta - \frac{R^2}{\zeta}\right) + \frac{\Gamma}{2\pi i} \log \frac{\zeta - \zeta_1}{\zeta + \bar{\zeta}_1} \frac{\zeta + R^2/\zeta_1}{\zeta - R^2/\bar{\zeta}_1} \quad . \tag{18}$$

Positive circulation is anti-clockwise looking upstream. Symmetry precludes the introduction of a vortex at the centre of the circle.

2.3 Implementing the conditions

We now wish to express the conditions at the separation lines and the conditions of zero overall force on each vortex system, as described in subsection 2.1, in equation form. By symmetry it is enough to consider the starboard half of the flow field. We have not so far specified how the vortex position Z_1 and circulation Γ are to depend on x, nor the shape of the separation line on the surface, though in Fig 2 both the vortex and the separation line are drawn as straight. This is the simplest possibility and corresponds to an inviscid flow which is conical and a quasi-conical boundary layer development. It agrees quite closely with observations of laterally symmetric flow on conical bodies provided (a) the state of the boundary layer at separation does not change along the length and (b) either the flow is supersonic or we are not too near the base of the cone if the flow is subsonic. For simplicity, we assume the lines are straight and the flow is conical, so that

$$\frac{dZ_1}{dx} = \frac{Z_1}{x} \quad \text{and} \quad \frac{d\Gamma}{dx} = \frac{\Gamma}{x} \quad . \tag{19}$$

The condition imposed by Bryson[1] at the separation line is that the flow there should be parallel to it. A rather more representative condition was investigated by Moore[2] and shown to affect the solution. However, it complicates the analysis, so, since our object is to find the effect of non-circular cross-sections, we retain the simple form of the separation condition. Since the separation line is straight, it can be specified by a constant value of τ:

$$\tau = s \ , \qquad y = a \cos s \ , \qquad z = b \sin s \ . \tag{20}$$

The direction ratios of the separation line are then

$$1 : a' \cos s : b' \sin s \ .$$

Hence, for the velocity vector to be parallel to this line

$$v - iw = Ua'(\cos s - i\tau \sin s) \ , \tag{21}$$

since the streamwise component of the disturbance velocity is small compared with U. The velocity is found from (18). Differentiating, we have

$$\frac{dW}{d\zeta} = \frac{\tau aa'U}{\zeta} - i\pi U\left(1 + \frac{R^2}{\zeta^2}\right) + \frac{\tau}{2\tau i}\left(\frac{1}{\zeta - \zeta_1} - \frac{1}{\zeta + \bar{\zeta}_1} + \frac{1}{\zeta + R^2/\zeta_1} - \frac{1}{\zeta - R^2/\bar{\zeta}_1}\right) \ . \tag{22}$$

From (3) and (14)

$$\frac{dW}{d\zeta} = (v - iw)\frac{dZ}{d\zeta} \ , \tag{23}$$

$$\zeta \frac{dZ}{d\zeta} = \zeta - \frac{a^2 - b^2}{4\zeta} = a(\tau \cos s + i \sin s) \tag{24}$$

at the separation line. Hence by (21), (23) and (24)

$$\zeta \frac{dW}{d\zeta} = Uaa'(\tau + i(1 - \tau^2) \cos s \sin s) \ . \tag{25}$$

Introducing $\zeta = Re^{is}$ into (22) and substituting the result into (25) gives an equation which reduces to

$$\frac{\tau(\zeta_1 + \bar{\zeta}_1)(\zeta_1\bar{\zeta}_1 - R^2)}{2\tau U(Re^{is} - \zeta_1)(Re^{is} + \bar{\zeta}_1)(Re^{-is} + \zeta_1)(Re^{-is} - \bar{\zeta}_1)} = \alpha + a'(1 - \tau) \sin s \ . \tag{26}$$

The final condition on which the model depends is that the system of the line-vortex and cut experiences no net force in the cross-flow plane. We consider the transverse forces acting on an element of length of each component of the starboard system, and represent them by complex quantities

$$\bar{\tau} = F_y + iF_z \quad , \tag{27}$$

where F_y and F_z are the components parallel to the y- and z-axes.

The magnitude of the force per unit length on the line-vortex is given by the product of the density, the circulation, and th fluid speed normal to the vortex. Its direction is normal to the vortex and normal to the fluid velocity, in the sense towards the side on which the speed is higher. The velocity component normal to the vortex arises partly from the small inclination of the vortex to the free stream, giving a contribution to the complex velocity of

$$-\frac{UZ_1}{x} \quad , \tag{28}$$

and partly from the velocity of the cross-flow at the position of the vortex. The complex conjugate of this velocity is given by

$$\lim_{Z \to Z_1} \frac{d}{dZ}\left(W - \frac{\Gamma}{2\pi i}\log(Z - Z_1)\right) \quad ,$$

since the self-induced velocity of the vortex is zero. The only term in W which is singular at $Z = Z_1$ is $(\Gamma/2\pi i)\log(\zeta - \zeta_1)$. Using a Taylor series for $Z - Z_1$ in terms of $\zeta - \zeta_1$, we find

$$\lim_{Z \to Z_1} \frac{d}{dZ}\left(\log(\zeta - \zeta_1) - \log(Z - Z_1)\right) = -\frac{d^2Z}{d\zeta^2}\Big/2\left(\frac{dZ}{d\zeta}\right)^2\Bigg|_{\zeta=\zeta_1}$$

Hence if the complex cross-flow velocity at the starboard vortex is $\bar{V}$, we have

$$\bar{V} = \frac{d\bar{\zeta}}{dZ}\left\{\frac{dW_a}{d\zeta} - \frac{\Gamma}{2\pi i}\left[\frac{1}{2}\frac{d^2Z}{d\zeta^2}\frac{d\zeta}{dZ} + \frac{\bar{\zeta}_1}{\zeta\bar{\zeta}_1 - R^2} + \frac{1}{\zeta + \bar{\zeta}_1} - \frac{\zeta_1}{\zeta\zeta_1 + R^2}\right]\right\} \quad , \tag{29}$$

evaluated at $\zeta = \zeta_1$. The complex force in the cross-flow plane per unit length of the starboard vortex is now

$$F_v = -i\rho\Gamma(\bar{V} - UZ_1/x) \quad . \tag{30}$$

The jump in velocity potential across the starboard cut is Γ . This gives rise to a jump in the longitudinal component of velocity of $d\Gamma/dx = \Gamma/x$, and so, through Bernoulli's equation, to a jump in pressure of $-\rho U\Gamma/x$, since the cross-flow component of velocity is continuous across the cut. The complex cross-flow force per unit streamwise length of the cut is therefore given by

$$F_c = i(Z_1 - a\cos s - ib\sin s)\rho U\Gamma/x \quad , \tag{31}$$

since the starboard separation line is at $Z = a\cos s + ib\sin s$. The condition of zero net force on the vortex and cut is just

$$F_v + F_c = 0 \quad . \tag{32}$$

Introducing (30) and (31) into (32) leads directly to

$$\frac{V}{U} = (2Z_1 - a\cos s - ib\sin s)/x \quad , \tag{33}$$

and the required condition follows by combining this with (29). The terms in (29) follow from (14)

$$\frac{dZ}{d\zeta} = 1 - \frac{a^2 - b^2}{4\zeta^2} \quad , \qquad \frac{d^2Z}{d\zeta^2} = \frac{a^2 - b^2}{2\zeta^3} \quad ,$$

and from (17)

$$\frac{dW_a}{d\zeta} = \frac{\tau aa'U}{\zeta} - i\alpha U\left(1 + \frac{R^2}{\zeta^2}\right) \quad .$$

Hence, after a little simplification, the condition is:

$$\frac{(2\bar{Z}_1 - a\cos s + ib\sin s)\left(4\zeta_1^2 - a^2 + b^2\right)}{4\zeta_1 x} = \tau aa' - i\alpha\left(\zeta_1 + \frac{R^2}{\zeta_1}\right) + \frac{i\Gamma}{2\pi U}\left[\frac{a^2 - b^2}{4\zeta_1^2 - a^2 + b^2} + \frac{R^2\zeta_1(\zeta_1 + \bar{\zeta}_1)}{\left(\zeta_1\bar{\zeta}_1 - R^2\right)\left(\zeta_1^2 + R^2\right)} + \frac{\zeta_1}{\zeta_1 + \bar{\zeta}_1}\right] \quad . \tag{34}$$

With Z_1 related to ζ_1 through the mapping (14), this is a complex equation connecting ζ_1 and Γ to the shape and incidence of the cone. Together with the real equation (26), it determines the vortex position and strength.

Before proceeding, we introduce non-dimensional variables and tidy up the notation. We extend the definition of δ used in section 1 so that it relates to the elliptic cone:

$$\delta = \frac{R}{x} \tag{35}$$

and introduce non-dimensional variables for the vortex position and strength:

$$\omega = \frac{\zeta_1}{R} , \qquad \gamma = \frac{\Gamma}{2\pi\delta UR} . \tag{36}$$

We note that, by (13) and (16)

$$a = \frac{2R}{1+\tau} , \qquad b = \frac{2R\tau}{1+\tau} ,$$

so that

$$a' = \frac{a}{x} = \frac{2\delta}{1+\tau} .$$

Then the condition (26) at the separation line becomes

$$\frac{\gamma(\omega\bar{\omega} - 1)(\omega + \bar{\omega})}{(e^{is} - \omega)(e^{is} + \bar{\omega})(e^{-is} + \omega)(e^{-is} - \bar{\omega})} = \frac{\alpha}{\delta} + 2\frac{1-\tau}{1+\tau}\sin s \tag{37}$$

and the condition (34) of zero net force becomes

$$\frac{2}{(1+\tau)^2}\left[(1+\tau)\bar{\omega} + \frac{1-\tau}{\bar{\omega}} - \cos s + i\tau \sin s\right]\left[(1+\tau)\omega - \frac{1-\tau}{\omega}\right]$$

$$= \frac{4\tau}{(1+\tau)^2} - i\frac{\alpha}{\delta}\left(\omega + \frac{1}{\omega}\right) + i\gamma\left[\frac{1-\tau}{(1+\tau)\omega^2 - 1 + \tau} + \frac{\omega(\omega + \bar{\omega})}{(\omega\bar{\omega} - 1)(\omega^2 + 1)} + \frac{\omega}{\omega + \bar{\omega}}\right] . \tag{38}$$

These equations, equivalent to three real equations, determine the position ω and strength γ of the starboard vortex in terms of the axis ratio τ, the incidence parameter α/δ, and the position, s, of the starboard separation line. γ can readily be eliminated, but numerical solution is required in general.

3 ANALYSIS FOR SMALL-SCALE SEPARATION

We now seek a solution of equations (37) and (38), assuming that the vortices are close to the separation lines, expecting to find that the vortices are weak. We follow the procedure used by Moore[2] for the circular cone. The first step is to rotate the axis system in the transformed plane, ζ, so that the starboard separation line lies on the real axis of the new plane. Then, if t is a non-dimensional complex coordinate of the starboard vortex in the new plane, we have

$$t = e^{-is}\zeta_1/R = \omega e^{-is} \tag{39}$$

and we seek a solution for t near unity. Following Moore, we choose the imaginary part of t as the small parameter ε, and assume the existence of a solution of the form

$$t = 1 + A\varepsilon + B\varepsilon^2 + \ldots + i\varepsilon \quad , \tag{40}$$

where the omitted terms are real and $o(\varepsilon^2)$.

We eliminate γ between (37) and (38) to give

$$\frac{2}{(1+\tau)^2}\left[(1+\tau)\bar{\omega} + \frac{1-\tau}{\bar{\omega}} - \cos s + i\tau \sin s\right]\left[(1+\tau)\omega - \frac{1-\tau}{\omega}\right]$$

$$= \frac{4\tau}{(1+\tau)^2} - i\frac{\alpha}{\delta}\left(\omega + \frac{1}{\omega}\right) + i\left[\frac{\alpha}{\delta} + 2\frac{1-\tau}{1+\tau}\sin s\right] \times$$

$$\times \frac{(e^{is} - \omega)(e^{is} + \bar{\omega})(e^{-is} + \omega)(e^{-is} - \bar{\omega})}{(\omega\bar{\omega} - 1)(\omega + \bar{\omega})} \times \left[\frac{1-\tau}{(1+\tau)\omega^2 - 1 + \tau}\right.$$

$$\left. + \frac{\omega(\omega + \bar{\omega})}{(\omega\bar{\omega} - 1)(\omega^2 + 1)} + \frac{\omega}{\omega + \bar{\omega}}\right] \quad . \tag{41}$$

Instead of regarding (41) as two real equations for the real and imaginary parts of ω for given τ and α/δ, we regard the equations as determining the real part of t and α/δ, for given $\mathrm{Im}\{t\} = \varepsilon$ and τ. So, in addition to the expansion (40), we assume an expansion of the form

$$\frac{\alpha}{\delta} = p + q\varepsilon + o(\varepsilon) \quad . \tag{42}$$

We note that ε may be negative, but $A\varepsilon$ in (40) is positive because the vortex lies outside the circle. Moore obtained a solution of this form for $\tau = 1$, so it is reasonable to seek one for general values of τ.

Most of the factors appearing in (41) are of order ε^0, but some are smaller. From (39) and (40)

$$\left.\begin{aligned} \omega &= e^{is}(1 + (A + i)\varepsilon + B\varepsilon^2 + \ldots) \\ \text{and so} \quad \omega\bar{\omega} - 1 &= 2A\varepsilon + (2B + A^2 + 1)\varepsilon^2 + \ldots \\ e^{is} - \omega &= -e^{is}\varepsilon(A + i + B\varepsilon + \ldots) \\ e^{-is} - \bar{\omega} &= -e^{is}\varepsilon(A - i + B\varepsilon + \ldots) \quad . \end{aligned}\right\} \tag{43}$$

Hence, in order to obtain the expansion of (41) to order ε, we need to consider the terms $O(\varepsilon^{-1})$ and $O(\varepsilon^0)$ in the final square bracket. We write these as

$$X = X_r + iX_i = \frac{1 - \tau}{(1 + \tau)e^{2is} - 1 + \tau} + \frac{\cos s + \varepsilon(A \cos s - \sin s)}{\varepsilon(2A + (2B + A^2 + 1)\varepsilon)(\cos s + (iA - 1)\varepsilon \sin s)} + \frac{e^{is}}{2 \cos s} \quad .$$

Some manipulation yields

$$X_r = \frac{1}{2A\varepsilon} + \frac{\tau}{2(\tau^2 \cos^2 s + \sin^2 s)} + \frac{A^2 - 2B - 1}{4A^2} \quad , \tag{44}$$

$$X_i = \frac{(\tau^2 - 1) \cos s \sin s}{2(\tau^2 \cos^2 s + \sin^2 s)} \quad . \tag{45}$$

The factor multiplying the final square bracket in (41) is purely imaginary, say iY, and we need the terms $O(\varepsilon)$ and $O(\varepsilon^0)$ in it. Introducing (42) and (43) we find, to this order,

$$Y = \varepsilon \frac{A^2 + 1}{A} \cos s \left(p + 2 \frac{1 - \tau}{1 + \tau} \sin s + q\varepsilon\right) \left(1 - \frac{(A^2 + 1)^2 + 2B(1 - A^2)}{2A(1 + A^2)} \varepsilon\right) \quad . \tag{46}$$

The first term on the right-hand side of (41) is real and independent of ε. The second term is, to the required order,

$$i\frac{\alpha}{\delta}\left(\omega + \frac{1}{\omega}\right) = 2ip\cos s - 2\varepsilon(Ap\sin s + ip\sin s - iq\cos s) \quad . \tag{47}$$

The left-hand side of (41) can be written as $2L/(1+\tau)^2$, where $L = L_r + iL_i$ and, after some manipulation, we find

$$L_r = 2\tau + 2A\varepsilon(1 + \sin^2 s + \tau^2(1 + \cos^2 s)) \quad , \tag{48}$$

$$L_i = (1 - \tau^2)\sin 2s + 2\varepsilon(\cos^2 s - 2\sin^2 s + \tau^2(\sin^2 s - 2\cos^2 s)) \tag{49}$$

to this order in ε. So, with (41) written as

$$\frac{2}{(1+\tau)^2}(L_r + iL_i) = \frac{4\tau}{(1+\tau)^2} - 2ip\cos s + 2\varepsilon(Ap\sin s + ip\sin s - iq\cos s) + iY(X_r + iX_i) \quad ,$$

its real and imaginary parts are

$$\frac{2}{(1+\tau)^2}L_r = \frac{4\tau}{(1+\tau)^2} + 2\varepsilon Ap\sin s - YX_i \quad , \tag{50}$$

$$\frac{2}{(1+\tau)^2}L_i = -2p\cos s + 2\varepsilon(p\sin s - q\cos s) + YX_r \quad . \tag{51}$$

Inspection of (50) with (48), (46) and (45) shows the $O(\varepsilon^0)$ term vanishes identically. The $O(\varepsilon^0)$ terms in (51) with (49), (46) and (44) give, after some re-arrangement:

$$(3A^2 - 1)\left(\frac{1-\tau}{1+\tau}\sin s + \frac{p}{2}\right)\cos s = 0 \quad . \tag{52}$$

The $O(\varepsilon)$ terms in (50) give, making use of the previous equations:

$$\frac{4A}{(1+\tau)^2}(1 + \sin^2 s + \tau^2(1 + \cos^2 s)) = 2Ap\sin s + \frac{A^2+1}{2A}\left(p + 2\frac{1-\tau}{1+\tau}\sin s\right)\times \times \frac{(1-\tau^2)\cos^2 s\sin s}{\tau^2\cos^2 s + \sin^2 s} \quad . \tag{53}$$

The left-hand side of (52) consists of three factors, one of which must vanish. We are not concerned with the possibility that $\cos s = 0$, that is to say that the separation lines lie in the plane of symmetry. If we suppose the middle factor vanishes, *ie*

$$p = -2\frac{1-\tau}{1+\tau}\sin s \quad ,$$

we find that (53) reduces to

$$\tau^2\cos^2 s + \sin^2 s + \tfrac{1}{2} = 0 \quad ,$$

which is impossible. Hence we must choose the remaining possibility:

$$A^2 = \frac{1}{3} \quad . \tag{54}$$

This agrees with Moore's result. Introducing it into (53) gives

$$(1+\tau)^2 p \sin s = 2\tau^2 + 4(\tau^2\cos^2 s + \sin^2 s)^2 \quad . \tag{55}$$

For the circular cone, $\tau = 1$, (55) reduces to

$$p = 1.5 \operatorname{cosec} s \quad ,$$

which agrees with Moore's result, and is Bryson's lower bound (1).

The $0(\varepsilon)$ terms in (51) are

$$\begin{aligned}\frac{4}{(1+\tau)^2}(c^2 - 2s^2 + \tau^2 s^2 - 2\tau^2 c^2) = {} & 2(ps - qc) + \frac{A^2+1}{A}c\left(p + 2\frac{1-\tau}{1+\tau}s\right) \\ & \times\left(\frac{\tau}{2(\tau^2c^2 + s^2)} + \frac{A^2 - 2B - 1}{4A^2}\right) \\ & + \frac{1}{2A}\frac{A^2+1}{A}cq - \frac{c}{2A^2}\left(p + 2\frac{1-\tau}{1+\tau}s\right)\times \\ & \times\frac{(A^2+1)^2 + 2B(1-A^2)}{2A} \quad ,\end{aligned} \tag{56}$$

where c and s have been written for $\cos s$ and $\sin s$. We see at once that when (54) is introduced, the term in q disappears from (56), so that q is not determined to this order. (56) is then a linear equation for B. Manipulation

is helped by introducing

$$E = \tau^2 c^2 + s^2 = \tau^2 \cos^2 s + \sin^2 s \qquad (57)$$

so that, from (55),

$$ps = \frac{2}{(1+\tau)^2}(\tau^2 + 2E^2) \quad , \quad p + 2\frac{1-\tau}{1+\tau}s = \frac{2E(2E+1)}{(1+\tau)^2 s}$$

while

$$(1-\tau^2)s^2 = E - \tau^2 \quad , \quad (1-\tau^2)c^2 = 1 - E \quad .$$

The solution emerges as

$$B = \frac{2}{9}\left(\frac{\tau}{E} - 3 + \frac{3A \tan s\ (2E^2 + 3E - 1)}{E(2E+1)}\right) \quad . \qquad (58)$$

When $\tau = 1$, $E = 1$ and (58) reduces to

$$B = \frac{4}{9}(2A \tan s - 1) \quad ,$$

which agrees with Moore's result for the circular cone.

We find γ , to first order in ε , from (37) and the equations of this section, as

$$\gamma = \frac{2E(2E+1)}{(1+\tau)^2} A\varepsilon \cot s \quad , \qquad (59)$$

where E is given by (57). As remarked above, $A\varepsilon > 0$, since the vortex is outside the body. Hence, since $E > 0$, γ has the sign of s , and, from (55), p and therefore α/δ have the sign of s . This means that the model represents weak vortices on the upper surface only, and the starboard vortex then induces anti-clockwise rotation when viewed from downstream.

At this stage it appears there are solutions for both positive and negative values of ε . However, there is a further condition to be applied to the solutions found so far. The condition which has been applied at the separation line is just that the velocity there is parallel to it. This condition is equally appropriate to an attachment line. The distinction between the two is that the surface flow converges onto a separation line and diverges away from an attachment line by continuity. This definition is deceptively simple and a more complete

discussion is planned for a subsequent report by the second and third authors. Fortunately, when the vortex lies close to the surface, the divergence or convergence is very strong, so that an intuitive approach gives the correct result. Define v_t as the component of the velocity in the cross-flow plane and tangential to the body cross-section, positive in the direction of ϕ increasing, *i.e.* anti-clockwise as viewed from downstream. Then, considering the neighbourhood of an attachment or separation line, on which the velocity vector is directed along the line, we see that if v_t is increasing with ϕ the surface streamlines are diverging, while if v_t is decreasing as ϕ increases the surface streamlines are converging.

If we write the real part of the complex potential W on the surface of the cone as the disturbance potential Φ, then $d\Phi/d\phi$ will be related to the tangential velocity, and a negative value of $d^2\Phi/d\phi^2$ will be associated with a separation line. Differentiating (18) we have

$$\frac{dW}{d\zeta} = \frac{\tau aa'U}{\zeta} - i\alpha U\left(1 + \frac{R^2}{\zeta^2}\right) + \frac{\Gamma}{2\pi i}\left(\frac{1}{\zeta - \zeta_1} - \frac{1}{\zeta + \bar{\zeta}_1} + \frac{1}{\zeta + R^2/\zeta_1} - \frac{1}{\zeta - R^2/\bar{\zeta}_1}\right) . \quad (60)$$

On the surface of the cone we write $\zeta = Re^{i\phi}$, with $\zeta_1 = R\omega$ and $\Gamma = 2\pi\delta UR\gamma$ as before, giving:

$$\frac{1}{U}\frac{dW}{d\zeta} = \frac{\tau aa'}{Re^{i\phi}} - i\alpha(1 + e^{-2i\phi}) - i\delta\gamma\left(\frac{1}{e^{i\phi} - \omega} - \frac{1}{e^{i\phi} + \bar{\omega}} + \frac{\omega}{\omega e^{i\phi} + 1} - \frac{\bar{\omega}}{\bar{\omega}e^{i\phi} - 1}\right) .$$

On the surface, $d\zeta = iRe^{i\phi}d\phi$, and so

$$\frac{1}{U}\frac{d\Phi}{d\phi} = \Re\left\{\frac{1}{U}\frac{dW}{d\phi}\right\} = \Re\left\{\frac{1}{U}\frac{dW}{d\zeta}\frac{d\zeta}{d\phi}\right\} =$$

$$2\alpha R\cos\phi + \delta R\gamma\left(\frac{e^{i\phi}}{e^{i\phi} - \omega} - \frac{e^{i\phi}}{e^{i\phi} + \bar{\omega}} + \frac{\omega}{\omega + e^{-i\phi}} - \frac{\bar{\omega}}{\bar{\omega} - e^{-i\phi}}\right) .$$

Hence, differentiating again,

$$\frac{1}{\delta UR}\frac{d^2\Phi}{d\phi^2} = -2\frac{\alpha}{\delta}\sin\phi + \gamma\left(-\frac{ie^{i\phi}\omega}{(e^{i\phi} - \omega)^2} - \frac{ie^{i\phi}\bar{\omega}}{(e^{i\phi} + \bar{\omega})^2} + \frac{ie^{-i\phi}\omega}{(\omega + e^{-i\phi})^2} + \frac{ie^{-i\phi}\bar{\omega}}{(\bar{\omega} - e^{-i\phi})^2}\right) .$$

.....(61)

We now write $\phi = s$, for the separation (or attachment) line in (61), and note that when the vortex is close to this line the dominant behaviour is that of the first and last terms in the large bracket. Hence, as $\varepsilon \to 0$,

$$\frac{1}{\delta UR}\frac{d^2\phi}{d\phi^2}\bigg|_s \sim \gamma i\left(\frac{\bar{\omega}e^{-is}}{(\bar{\omega} - e^{-is})^2} - \frac{\omega e^{is}}{(\omega - e^{is})^2}\right)$$

$$\sim \gamma i\left(\frac{1}{(A - i)^2\varepsilon^2} - \frac{1}{(A + i)^2\varepsilon^2}\right) \qquad \text{by (43)}$$

$$= -\frac{4A\gamma}{(A^2 + 1)^2\varepsilon^2}$$

$$\sim -\frac{3E(2E + 1)\cot s}{2(1 + \tau)^2\varepsilon} \qquad \text{by (54) and (59).}$$

By (57) $E > 0$, so $\phi = s$ is a separation line if ε has the sign of s, and an attachment line otherwise. Taking $\alpha/\delta > 0$ without loss of generality, so that the previous argument shows $s > 0$, we find separation corresponds to $\varepsilon > 0$. This means the vortex lies to leeward of the separation line, as would be expected.

In the hope of clarifying the roles of the solutions with ε positive and negative, we use the formal solution to express, for a given separation line, $\phi = s$, first the nearby vortex position corresponding to a small positive value of ε, and then the nearby attachment line associated with the presence of the vortex. Suppose the attachment line is at $\phi = \bar{a}$. Then, regarding (43) as relating the vortex position ω to the separation line, we have

$$\omega = e^{is}(1 + (A + i)\varepsilon + B\varepsilon^2 + \ldots),$$

where, since $\varepsilon > 0$, $A > 0$ and $A = |A|$. Now, regarding (43) as relating the same vortex position to the attachment line, with a small parameter $\bar{\varepsilon} < 0$, we have

$$\omega = e^{i\bar{a}}(1 + (A + i)\bar{\varepsilon} + B\bar{\varepsilon}^2 + \ldots),$$

where, since $\bar{\varepsilon} < 0$, $A < 0$ and $A = -|A|$. Hence, equating the expressions for ω:

$$e^{i\bar{a}}(1 - |A|\bar{\varepsilon} + i\bar{\varepsilon} + B\bar{\varepsilon}^2 + \ldots) = e^{is}(1 + |A|\varepsilon + i\varepsilon + B\varepsilon^2 + \ldots) \quad .$$

Taking logarithms of both sides and expanding $\log(1 + x)$ for small x, we have

$$i\bar{a} - |A|\bar{\varepsilon} + i\bar{\varepsilon} + B\bar{\varepsilon}^2 - \tfrac{1}{2}(-|A|\bar{\varepsilon} + i\bar{\varepsilon})^2 + \ldots = is + |A|\varepsilon + i\varepsilon + B\varepsilon^2 - \tfrac{1}{2}(|A|\varepsilon + i\varepsilon)^2 \quad .$$

The real part of this equation shows that

$$\bar{\varepsilon} = -\varepsilon(1 + O(\varepsilon^2)) \tag{62}$$

and the imaginary part shows that

$$\bar{a} = s + 2\varepsilon(1 - |A|\varepsilon) \quad , \tag{63}$$

where $|A| = 1/\sqrt{3}$.

This situation is sketched in the plane of ω in Fig 3a for $\varepsilon = 0.1$. To graphical accuracy the term $B\varepsilon^2$ is negligible for the separation position $s = 30^\circ$ shown. The positions of the separation line, attachment line and vortex are indicated by the letters S, A and V, and lengths ε and $A\varepsilon$ are marked. The corresponding configuration in the physical cross-flow plane Z is sketched in Fig 3b for $\tau = 0.5$. The points S, A and V are in their calculated positions, but the separating conical streamline SV and attaching conical streamline meeting the surface at A are guessed. The arrows show the convergence of the surface flow onto S and divergence from A .

4 ANGLE OF INCIDENCE FOR VORTEX FORMATION

As explained in the Introduction, for circular cones the value of α for which vortices first appear at the surface of the cone provides a lower bound to the angles of incidence for which the model has solutions, as long as the separation line is to leeward of a critical position, $\theta_c \doteq 46^\circ$. For separation positions further to windward, there are unstable solutions for lower angles of incidence, but the incidence for which vortices first appear at the surface is still of interest.

For elliptic cones equations (42) and (55) show that this angle of incidence is given by:

$$\frac{\alpha}{\delta} = p = \frac{2\tau^2 + 4(\tau^2 \cos^2 s + \sin^2 s)^2}{(1 + \tau)^2 \sin s} \quad , \tag{64}$$

where $\tau = b/a$, $\delta = R/x = \frac{1}{2}(a + b)/x = \frac{1}{2}(1 + \tau)a'$, and the separation line is $y = a \cos s$, $z = b \sin s$. In this section we discuss the dependence of α on τ and s . The elliptic cones include the circular cone, $\tau = 1$, and the flat-plate delta wing, $\tau = 0$. For a slender circular cone, δ is just the semi-angle at the apex, so that α/δ is a natural ratio to consider for cones not too far from circular. For a flat-plate wing, it is more natural to relate the angle of incidence to the semi-angle of the wing apex, which is a' if the wing is slender, so we also consider the behaviour of

$$\frac{\alpha}{a'} = \frac{\alpha}{\delta}\frac{1 + \tau}{2} = \frac{\tau^2 + 2(\tau^2 \cos^2 s + \sin^2 s)^2}{(1 + \tau) \sin s} \quad . \tag{65}$$

Fig 4 shows the variation of α/a' with separation position for the circular cone and the flat plate. The variations, given by 1.5 cosec s and $2 \sin^3 s$, respectively, could hardly be more different. The curve for the circular cone is familiar, showing the angle of incidence needed for vortex formation increases as the separation line moves to windward. The curve for the flat-plate delta is believed to be new. It shows there are solutions for all angles of incidence for separation at the leading edge, $s = 0$, as is well-known, though for very small values of α/a' their behaviour is unphysical[8]. Since separation will take place at a sharp leading edge, there seems little reason to consider other values of s . However, Wood and Roberts[9] have shown that blowing tangentially to the upper surface of a thin delta wing from a slot near the rounded leading edge, in an inboard direction, delays the onset of separation and vortex formation to larger angles of incidence. Since the effect of blowing is to move the separation line inboard, the behaviour of this simple model, as illustrated in Fig 4, is consistent with their observations.

The most dramatic difference between the curves in Fig 4 is at the small values of s . Equation (64) shows that, as $s \to 0$, α/δ increases without limit unless τ is zero, when $\alpha/\delta \to 0$. It is not surprising that the behaviour is non-uniform near the point $s = \tau = 0$ of the parameter space, since the inclination of the surface at the leading edge changes abruptly through 90° as τ reaches zero. Fig 5 shows how the variation of α/a' with s changes as τ increases from zero to unity. For the lower values of τ ($\tau^2 < 2/3$) , the curves have a minimum at a value of s less than 90°, with a local maximum at 90°. For larger values of τ there is a minimum at $s = 90^\circ$.

The bunching together of the curves for s near 90° is resolved in Fig 6, by plotting α/δ instead of α/a' . Each curve retains its shape, but its

relation to the others changes. Also included in Fig 6 are curves for values of τ greater than unity, that is to say, for cones deeper than they are wide. The particular values of τ chosen correspond to the same cones as before, but rolled through 90°. As τ increases above unity, the angle of incidence needed for vortex formation increases steadily, except for values of s near 90°. The general trend exhibited in Figs 4 to 6 is for the region in which solutions exist to become confined to the larger angles of incidence as the thickness ratio increases, except for separation positions well to leeward, where the tendency can be reversed to a limited extent.

No attempt is made to discuss the results in terms of the typical positions of separation observed in laminar or turbulent flow. The reason for not doing so emerges from a consideration of Fig 7. This compares vortex sheet and line-vortex solutions for a circular cone at $\alpha/\delta = 3$. The vortex sheet solution is calculated by the method of Fiddes[10]. The separation line for the sheet, S_s, is at $s = 0^{\circ}$, a convenient value typical of laminar boundary layer separation. The sheet extends to E, and is joined to the core C by a feeding sheet represented by a broken line. The arc labelled '40° to 49°' represents the vortex positions in the line-vortex model for separation positions $40^{\circ} \leqslant s \leqslant 49^{\circ}$. It is apparent that, with $s = 45^{\circ}$, the line-vortex model gives almost the same vortex position as the vortex sheet model gives with $s = 0$. The non-dimensional circulation, ν, of the line-vortex for $s = 45^{\circ}$ is 1.299, and the point B on the vortex sheet has been chosen so that the circulation of the combination of the vortex core at C and the sheet between B and E is also 1.299. The initial behaviour of the conical streamline separating from S_v, at $s = 45^{\circ}$, is sketched.

This suggests that the line-vortex model can produce solutions resembling those of the vortex-sheet model if the separation position is displaced to leeward. We plan to present more evidence for this later. A partial explanation for this is the different behaviour of the two models near the separation line. For the sheet model the flow leaves the surface tangentially, the sheet remaining close to the body for some distance before turning away from it and beginning to wrap around the core. For the line-vortex model the separation stream surface (or conical streamline) leaves the surface at right angles. Thus similar global flow patterns are produced by the two models if the separation line in the line-vortex model is displaced to leeward. There is evidence that the vortex-sheet model gives vortex positions in reasonable agreement with experiment (the occurrence of secondary separation prevents close agreement) when observed separation positions are used, so it would not be appropriate to use observed separation positions in the line-vortex model.

5 CONCLUSIONS

The single line-vortex model of laterally symmetric separation from a circular cone at incidence has been extended to elliptic cones. Analytical solutions have been obtained for the case in which the vortices are weak and lie close to the surface of the cone. In particular, the well-known result of Bryson[1] for the angle of incidence at which the vortices first appear adjacent to specified separation lines on a circular cone has been extended to elliptic cones.

This shows that, for separation lines not too close to the leeward generator, the effect of reducing the vertical axis of the cross-section, that is, of making the body more wing-like, is to reduce the angle of incidence at which the vortices first appear. If the separation lines are close to the leeward generator, the thinner bodies require large angles of incidence to produce vortices. If the vertical axis is made larger than the horizontal axis, the angle of incidence for the appearance of vortices increases, unless the separation lines are well to leeward.

In the limit of zero thickness ratio, when the body becomes a flat-plate delta wing, the familiar behaviour of the wing solution is recovered, but the limit is not approached uniformly.

LIST OF SYMBOLS

a	horizontal semi-axis of elliptic cross-section
$\bar{a}$	value of ζ at attachment line
A	coefficient in expansion (40)
b	vertical semi-axis of elliptic cross-section
B	coefficient in expansion (40)
D	see equation (10)
E	see equation (57)
F	complex force
$\mathrm{Im}\{\ \}$	imaginary part
L	group of terms in equation (41), see (48) and (49)
p,q	coefficients in expansion (42)
R	$\frac{1}{2}(a + b)$, radius of circle
$\mathrm{Re}\{\ \}$	real part
s	value of ζ at starboard separation line
S	function defining body surface
t	complex variable, equation (39)
U	free-stream speed
v,w	components of velocity parallel to y,z axes
v_n	component of velocity in cross-flow plane, normal to body cross-section
v_{n_ζ}	component of velocity normal to circle in ζ-plane
V	complex velocity, $v + iw$
W	complex potential
x,y,z	Cartesian coordinates, see Figs 1 and 2
X,Y	groups of terms in (41), see (44) to (46)
Z	complex variable in cross-flow plane
α	angle of incidence
Γ	non-dimensional circulation, equation (36)
γ	circulation of starboard vortex
δ	semi-apex-angle of circular cone, more generally, R/x
ε	$\mathrm{Im}\{t\}$, small
$\bar{\varepsilon}$	value of ε for attachment line
ζ	complex variable in circle plane
θ_s	position of separation line on circular cone, see Fig 1
ρ	density
τ	a/b, axis ratio of elliptic cross-section

LIST OF SYMBOLS (concluded)

ϕ	angular coordinate on ellipse
Φ	disturbance potential on surface
ζ	non-dimensional position of vortex in ζ-plane

suffixes

a	attached flow
c	cut
i	imaginary part
r	real part
v	vortex
l	starboard vortex

REFERENCES

No.	Author	Title, etc
1	A E Bryson	Symmetric vortex separation on circular cones. *J. Appl. Mech. (ASME)*, 26, 643-6 (1959)
2	Katharine Moore	Line-vortex models of separated flow past a circular cone at incidence. Unpublished MoD material, 1981
3	M. Pidd J.H.B. Smith	Asymmetric vortex flow over circular cones. AGARD Conference on Vortex Flow Aerodynamics, Scheveningen, October 1990
4	D.E. Dyer S.P. Fiddes J.H.B. Smith	Asymmetric vortex formation from cones at incidence - a simple inviscid model. *Aeron. Quart.*, 33, 293-312 (1982), also RAE Technical Report 81130 (1981)
5	S.P. Fiddes J.H.B. Smith	Calculations of asymmetric separated flow past circular cones at large angles of incidence. Paper 14 in Missile Aerodynamics, AGARD-CP-336, 1982
6	F. Marconi	Asymmetric separated flows about sharp cones in a supersonic stream. 11th Int. Conf. Num. Meth. Fluid. Dyn., Williamsburg, 1988; Lecture Notes in Physics No.323, Springer, 1989
7	M.J. Siclari F. Marconi	The computation of Navier-Stokes solutions exhibiting asymmetric vortices. AIAA Paper 89-1817 (1989)
8	J.H.B. Smith	The isolated-vortex model of leading-edge separation revised for small incidence. RAE Technical Report 73160 (1974)
9	N.J. Wood L. Roberts	Control of vortical lift on delta wings by tangential leading-edge blowing. *J. Aircraft*, 25, 3, 236-243 (1988)
10	S.P. Fiddes	A theory of the separated flow past a slender elliptic cone at incidence. In Computation of Viscous-Inviscid Interactions, AGARD-CP-291, 1980

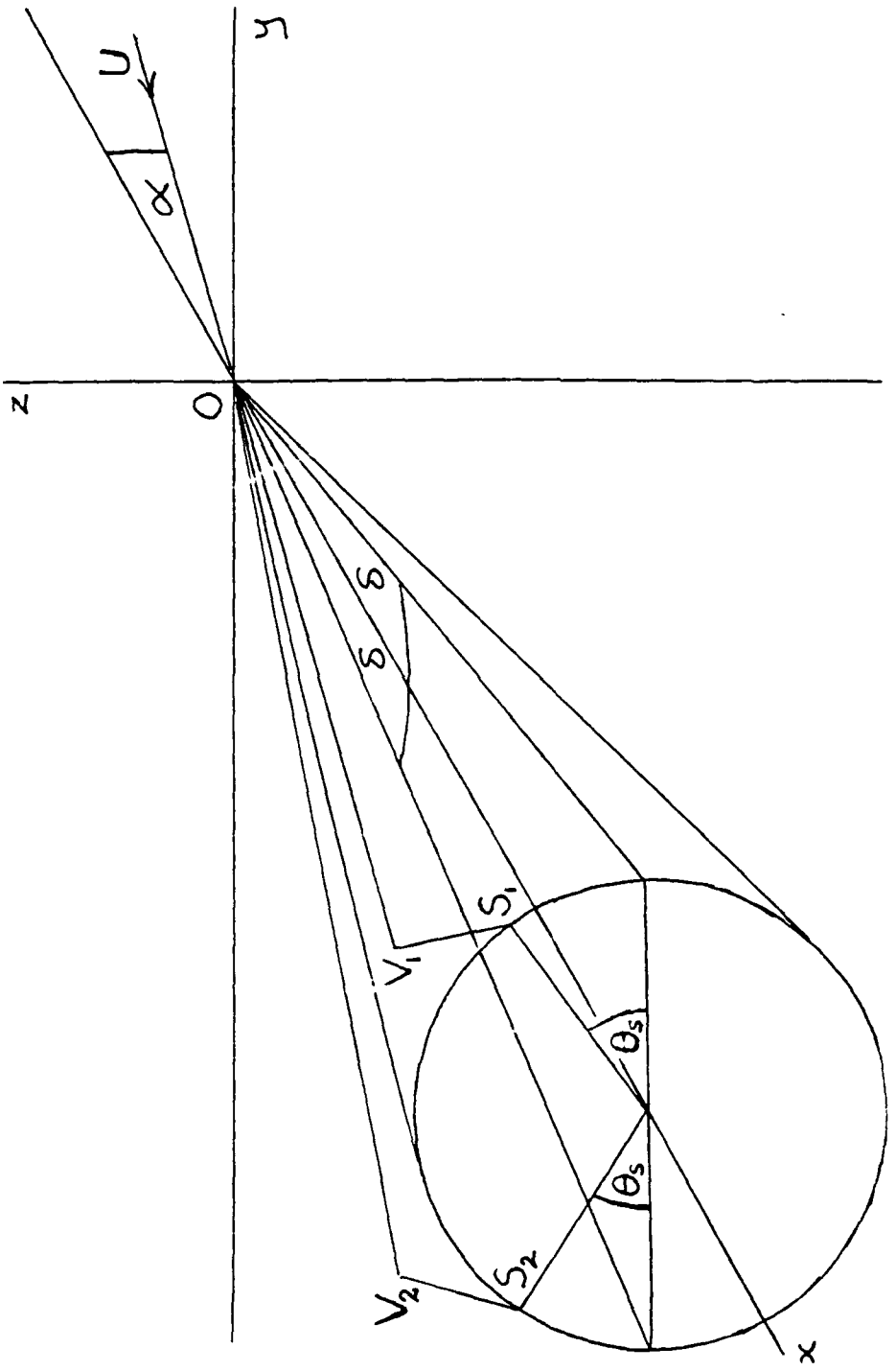

Fig 1 Definition sketch for circular cone

Fig 2

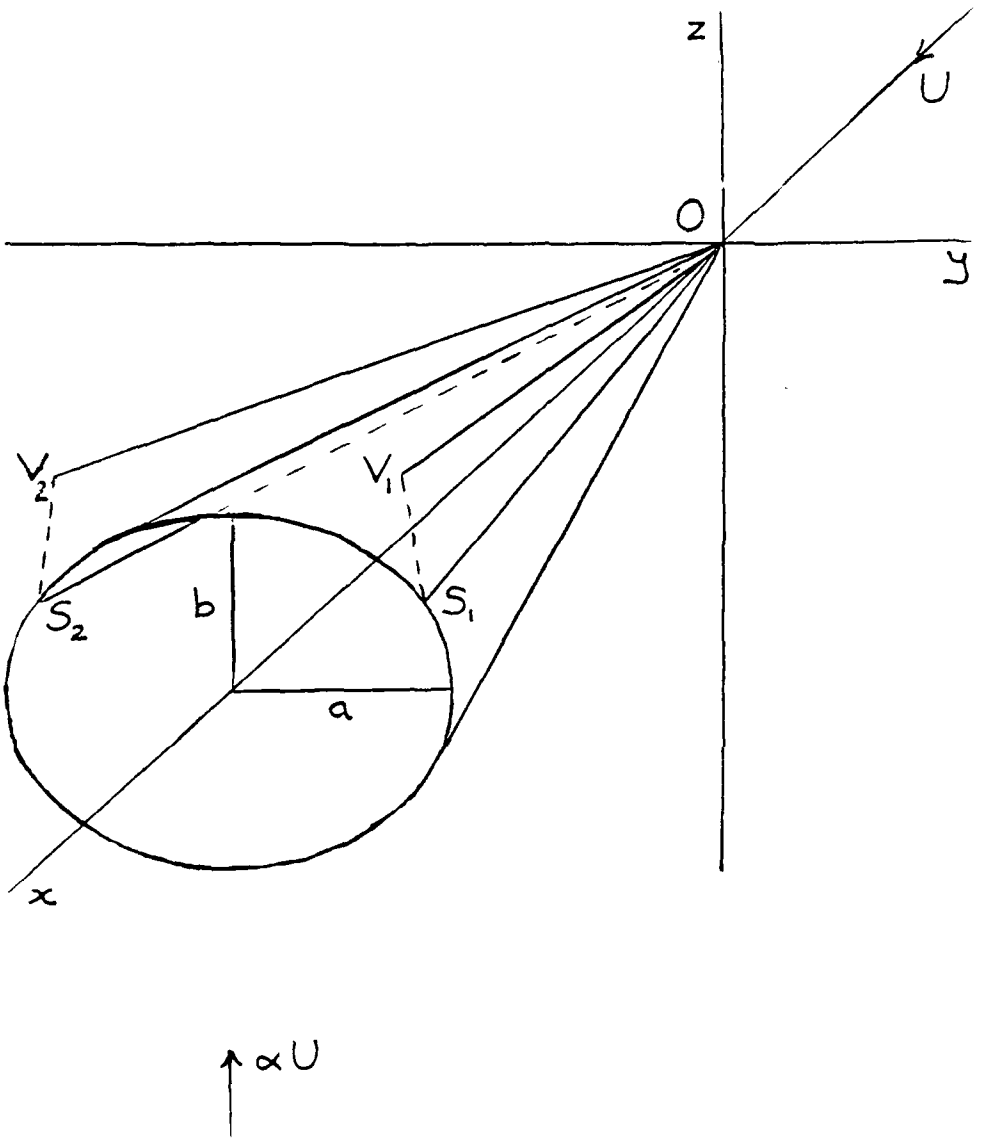

Fig 2 Definition sketch for elliptic cone

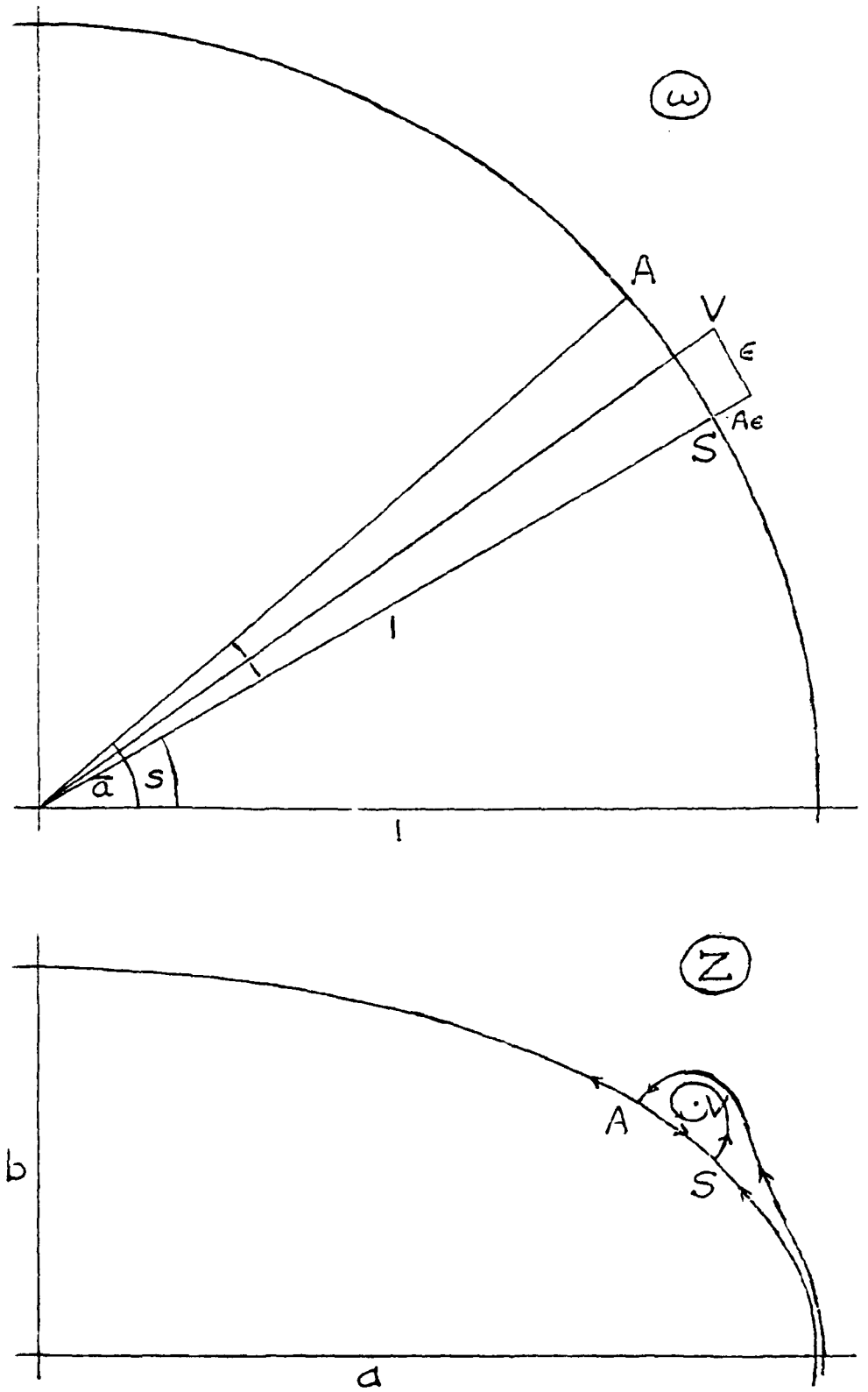

Fig 3 Relation of weak vortex to separation and attachment lines

Fig 4

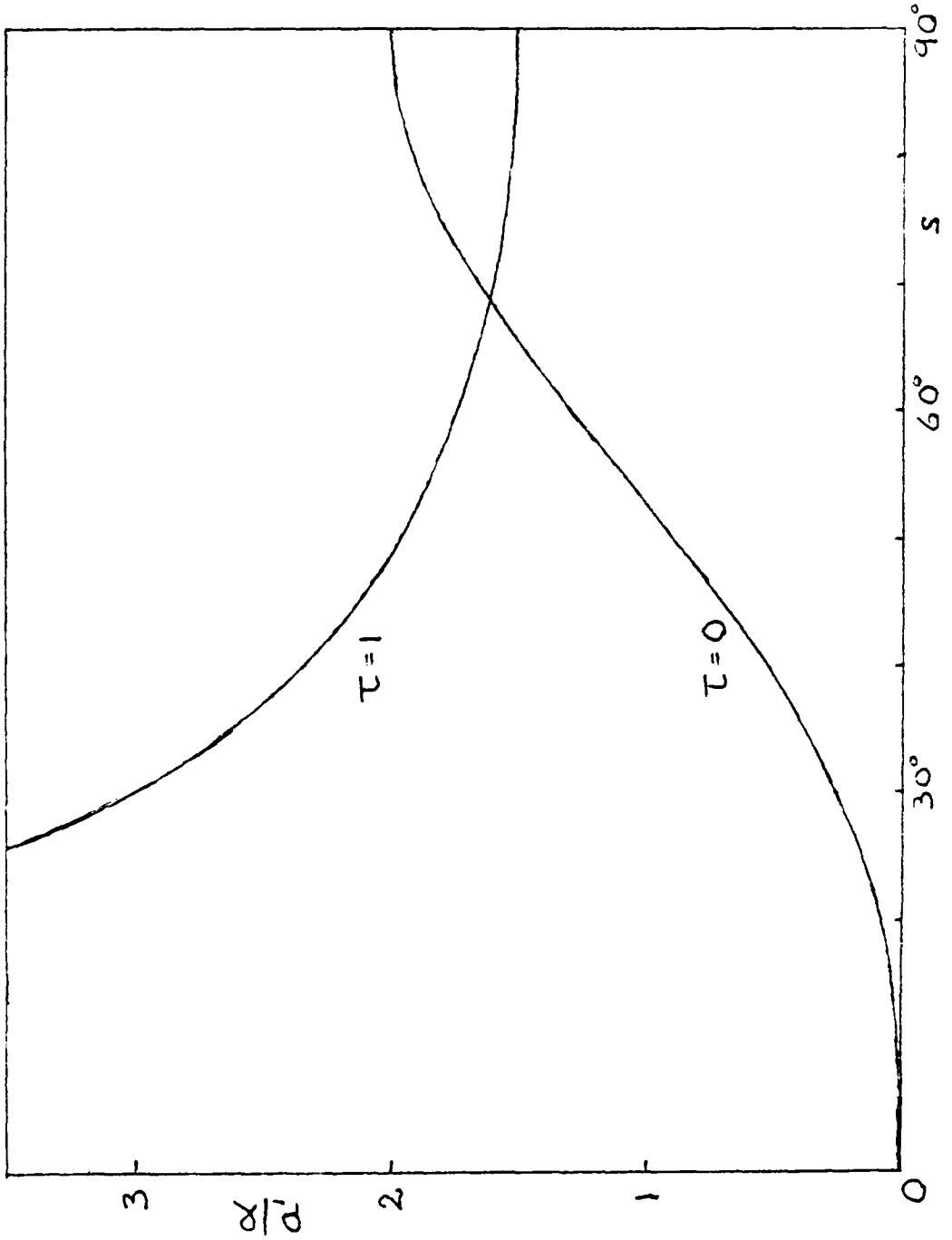

Fig 4 Ratio of incidence to planform semi-angle for initial vortex formation on flat delta and circular cone as a function of separation position

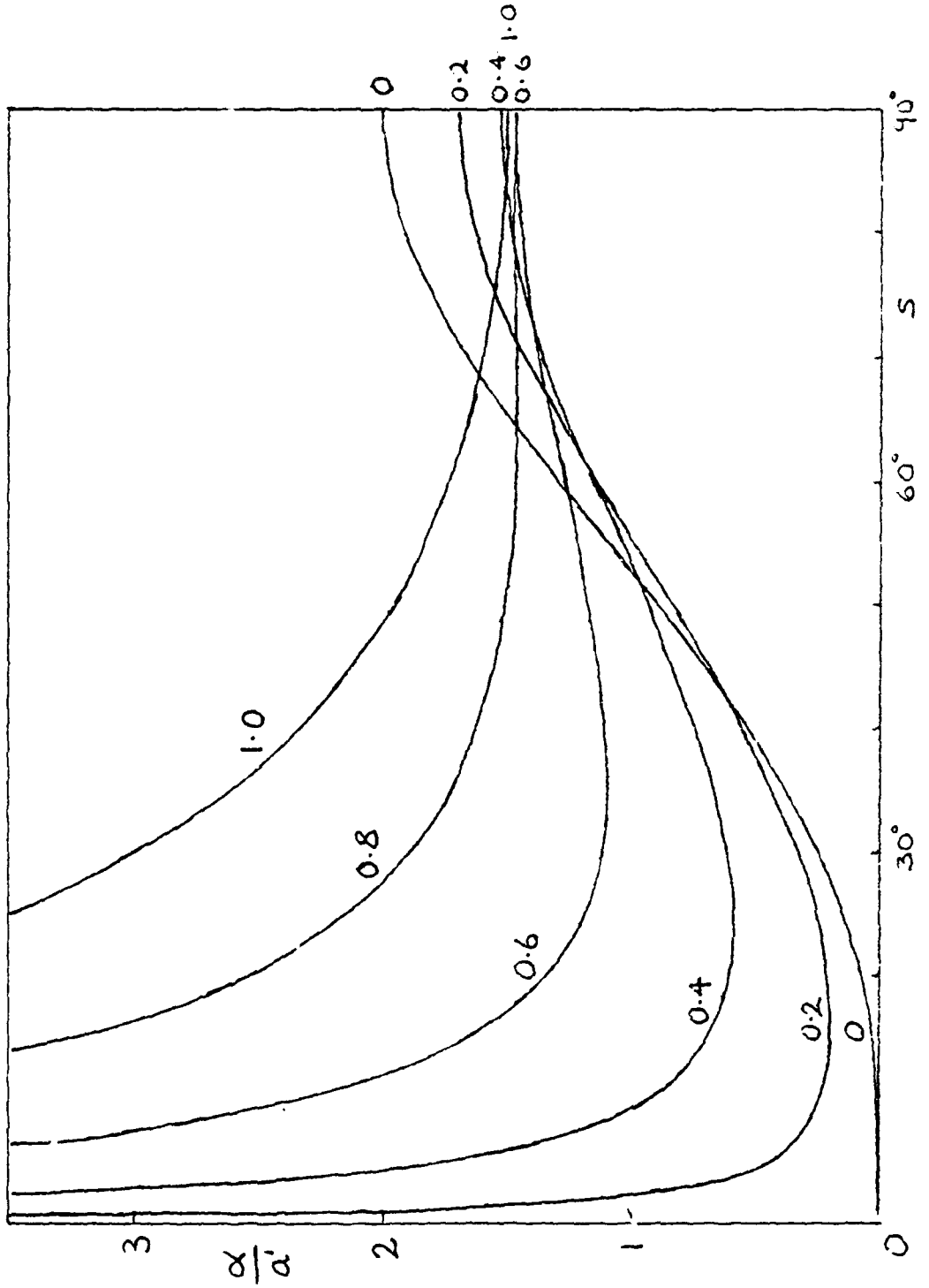

Fig 5 Ratio of incidence to planform semi-angle for initial vortex formation for various axis ratios up to unity

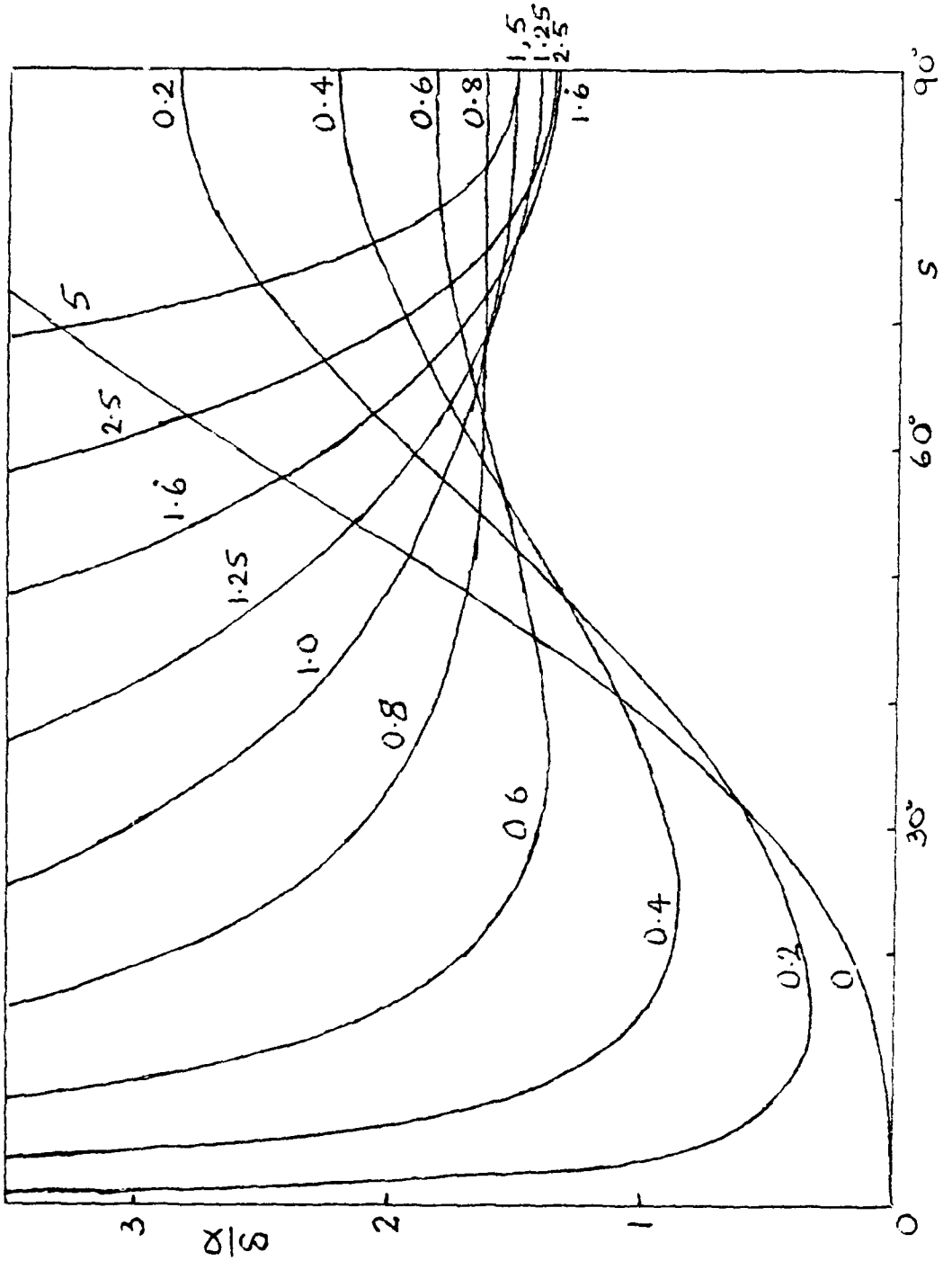

Fig 6 Ratio of incidence to average semi-angle at nose for initial vortex formation for various axis ratios

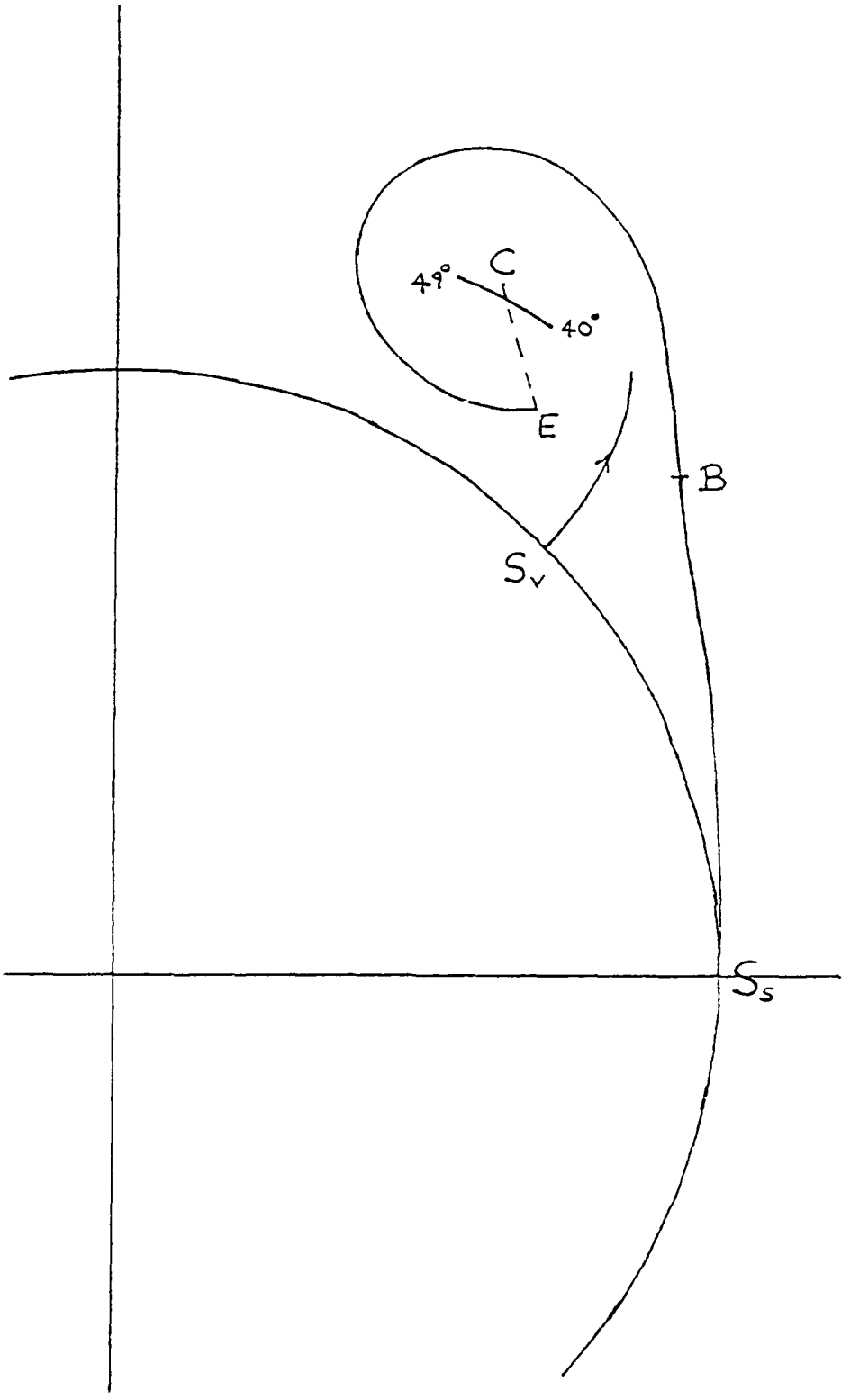

Fig 7 Relation between vortex-sheet and line-vortex solutions, $\alpha/\delta = 3$

REPORT DOCUMENTATION PAGE

Overall security classification of this page

UNLIMITED

As far as possible this page should contain only unclassified information. If it is necessary to enter classified information, the box above must be marked to indicate the classification, e.g. Restricted, Confidential or Secret.

1. DRIC Reference (to be added by DRIC)	2. Originator's Reference	3. Agency Reference	4. Report Security Classification/Marking
	RAE TM Aero 2197		UNLIMITED

5. DRIC Code for Originator	6. Originator (Corporate Author) Name and Location
7673000W	Royal Aerospace Establishment, Farnborough, Hants, UK
5a. Sponsoring Agency's Code	6a. Sponsoring Agency (Contract Authority) Name and Location

7. Title: A simple model of vortex flow past a slender elliptic cone at incidence

7a. (For Translations) Title in Foreign Language

7b. (For Conference Papers) Title, Place and Date of Conference
N/A

8. Author 1. Surname, Initials	9a. Author 2	9b. Authors 3, 4	10. Date	Pages	Refs.
Pinkney, Joanne	Pidd, M	Smith J.H.B.	October 1990	34	10

11. Contract Number	12. Period	13. Project	14. Other Reference Nos.
		N/A	

15. Distribution statement
(a) Controlled by – Head of Aerodynamics Department, RAE

(b) Special limitations (if any) –

If it is intended that a copy of this document shall be released overseas refer to RAE Leaflet No.3 to Supplement 6 of MOD Manual 4.

16. Descriptors (Keywords) (Descriptors marked * are selected from TEST)

Vortices*. Boundary layer separation*. Slender-body theory.

17. Abstract

The single line vortex model of the separated flow past a slender pointed body of revolution at incidence is extended to elliptic cones, within the framework of slender-body theory, and maintaining lateral symmetry in the flow. An analytical solution is found for the limiting behaviour of the model when the vortices are weak. The angle of incidence above which solutions exist is found as a function of the axis ratio of the elliptic cross-section and the postulated location of the separation lines.

F5910/1

RAE Form A143 (revised October 1980)